High-order algorithms for large-eddy simulation of incompressible flows

R. PASQUETTI[1], C.J. XU[2]
[1] Lab. J.A. Dieudonné, UMR CNRS 6621, University of Nice-Sophia Antipolis, 06108 Nice, France
[2] Dpt of Mathematics, University of Xiamen, 361005 Xiamen, Fujian, China

Abstract

"Defiltering-Transport-Filtering" (DTF) algorithms are proposed for the large eddy simulation of incompressible flows by using high order methods. These new algorithms are based (i) on an approximate deconvolution method for the modeling of the sub-grid scale stress tensor and (ii) on a semi-Lagrangian method to handle the convective term. Such algorithms are implemented in 3D spectral solvers (one homogeneous direction), using differential operators to handle in an approximate way the filtering and defiltering operations. Stability and dissipation properties of the schema are discussed. Preliminary results, obtained with a Chebyshev collocation solver, for the 3D wake of a cylinder with Reynolds number equal to 1000 are presented.

Key words: Large Eddy Simulation, incompressible flows, Spectral methods.

1 Introduction

The LES (Large Eddy Simulation) equations for incompressible flows are obtained by applying a spatial filtering to the incompressible Navier-stokes equations (see e.g [14]). When assuming that the filtering operator and the spatial derivatives commute one obtains:

$$\begin{cases} \partial_t \bar{\boldsymbol{u}} + \nabla \cdot (\bar{\boldsymbol{u}} \otimes \bar{\boldsymbol{u}}) = -\nabla \bar{p} + \nu \nabla^2 \bar{\boldsymbol{u}} - \nabla \cdot \tau \\ \nabla \cdot \bar{\boldsymbol{u}} = 0 \end{cases} \tag{1}$$

where a bar is used to specify the filtered quantities, i.e. $\bar{\boldsymbol{u}} = (\bar{u}_1, \bar{u}_2, \bar{u}_3)$ and $\bar{p}$ are the filtered velocity and pressure respectively:

$$\bar{u}_i = G u_i \quad and \quad \bar{p} = G p \tag{2}$$

with G a convolution operator characterized by its kernel, i.e by a filter function of filter width Δ in physical or spectral space [15, 20].

Similarly to the RANS (Reynolds Averaged Navier-Stokes) equations, the non-linear convective term yields an additional tensor in the momentum equation. It is the so-called subgrid-scale stress (SGS) tensor τ, such that:

$$\tau_{ij} = \overline{u_i u_j} - \bar{u}_i \bar{u}_j \tag{3}$$

Then occurs a closure problem: the tensor τ must be modelled.

Closure of the filtered Navier-Stokes equations can be handled in several ways and SGS modeling remains a serious problem. Hereafter we follow an approach of the "velocity estimation model" or "Approximate Deconvolution Method" (ADM) type [2, 3, 21, 22].

Deconvolution problems being ill-posed, the idea of the ADM is to introduce an approximate inverse of the convolution operator, to get from the filtered velocity an approximation of the exact velocity which then can be used for the determination of the SGS tensor τ:

$$\tau_{ij} = \overline{u_i^\star u_j^\star} - \bar{u}_i^\star \bar{u}_j^\star \quad where \quad u_i^\star = G^+ \bar{u}_i \tag{4}$$

with G^+, the "defiltering operator", i.e. an approximate inverse of G.

Here one may remark that with $G^+ = 1$ (1, identity operator) one recovers the following form of the scale similarity model [1]:

$$\tau_{ij} = \overline{\bar{u}_i \bar{u}_j} - \bar{u}_i \bar{u}_j \tag{5}$$

where the "test-filter" is only formally the same as that the filter used to obtain the filtered quantities. Thus, it may be considered that the ADM essentially yields improved scale similarity type models.

Scale similarity models are known to be not enough dissipative but better on "*a priori* tests" than "Eddy viscosity models", which generally state a proportionality between the deviatoric part of the SGS tensor, say τ_{ij}^D, and of the filtered strain rate tensor:

$$\tau_{ij}^D = -2\nu_T \bar{S}_{ij} \tag{6}$$

with $\bar{S}_{ij} = \frac{1}{2}(\partial_i \bar{u}_j + \partial_j \bar{u}_i)$ and ν_T an eddy viscosity, e.g. $\nu_T = (C_s \Delta)^2 |\bar{S}|$, Δ filter width, C_S the Smagorinsky constant.

Mixed models, i.e. which use both the eddy viscosity and the scale similarity concepts, are probably the most efficient. In any cases, improvements may also be found out by using the dynamic modeling [7], based on a double filtering to determine the optimal values of the control parameters of the SGS model.

The starting point of the present study is the ADM approach recently proposed in [12], which makes use of Taylor expansions of the u_i to get approximations of the filter and of its inverse. Thus, with 3D filters defined as the tensorial product of 1D Gaussian or "box" convolution kernels of filter widths Δ_i in direction i, with a $O(\Delta_1^4, \Delta_2^4, \Delta_3^4)$ approximation one obtains:

$$\begin{aligned} G &= 1 + A \\ G^+ &= 1 - A \end{aligned} \tag{7}$$

where $A = \dfrac{1}{24} \displaystyle\sum_{i=1}^{3} \Delta_i^2 \partial_i^2$.

The authors mention that such a model shows the advantage of having no free parameter, but that the Δ_i must be taken greater than twice the size of the grid spacing h_i.

Of course, the filter width is generally not constant, especially if an "implicit filtering" by a non-homogeneous computational grid is assumed. Consequently, the previous expression of A is approximative and moreover the convolution and differential operators no-longer commute, so that a commutation error arises in the LES equations. In this paper we do not address this problem, assuming that the space variations of the grid size are "sufficiently smooth" to allow us to neglect all the extra-terms arising from these space variations [9].

Knowing that Δ is $O(h)$, the present approach again shows that using low order methods (i.e. not better than $O(h^2)$) for LES is questionable, since approximation errors and SGS modeling adjustments may show comparable amplitudes [9, 13].

2 Defiltering-Transport-Filtering algorithms

Spectral solvers are usually based on semi-implicit time-schemes: Linear terms are treated implicitly and non-linear ones explicitly, using an Adams-Bashforth extrapolation. When high Reynolds number flows are concerned, for stability reasons it is of interest to look for alternative procedures. One of them is the "semi-Lagrangian" method, defined as a result of the operator-integration-factor splitting method in [17], which permits an efficient computation of the solution at the feet of the characteristics issued from the grid-points before solving a generalized Stokes problem [18, 25]. The specificity of this semi-Lagrangian approach is that no high-order spatial interpolations are required, which is essential in the frame of spectral methods.

The basic idea of the DTF algorithms is to combine the ADM with this semi-Lagrangian method. To this end we first rewrite the filtered incompressible Navier-Stokes equations in convective form:

$$\begin{cases} \overline{D_t \boldsymbol{u}} = -\nabla \bar{p} + \nu \nabla^2 \bar{\boldsymbol{u}}, \\ \nabla \cdot \bar{\boldsymbol{u}} = 0 \end{cases} \tag{8}$$

where D_t stands for the material derivative. The approximation of $D_t \boldsymbol{u}$ with a BDQ approximation (Backward Differentiation of order Q) yields, with $\alpha_q, q = 1, \cdots, Q$, a set of given coefficients:

$$D_t \boldsymbol{u} = \frac{1}{\Delta t}(\alpha_0 \boldsymbol{u}^{n+1} + \sum_{q=1}^{q=Q} \alpha_q \tilde{\boldsymbol{u}}^{n+1-q}) + O(\Delta t^Q) \tag{9}$$

where $\boldsymbol{u}^{n+1} \approx \boldsymbol{u}(\boldsymbol{x}, t_{n+1})$ and $\tilde{\boldsymbol{u}}^{n+1-q} \approx \boldsymbol{u}(\boldsymbol{\chi}(\boldsymbol{x}, t_{n+1}; t_{n+1-q}), t_{n+1-q})$, with $\boldsymbol{\chi}(\boldsymbol{x}, t_{n+1}; t)$ the characteristic issued from $(\boldsymbol{x}, t_{n+1})$. Note that the $\tilde{\boldsymbol{u}}^{n+1-q}$, $q = 1, \cdots, Q$, are nothing but the consecutive values of $\boldsymbol{u}$ at times t_{n+1-q} when following the fluid particle passing at $\boldsymbol{x}$ at time t_{n+1}. Applying now the filtering operator G to this BDQ approximation of the material derivative one obtains:

$$\overline{D_t \boldsymbol{u}} \approx \frac{1}{\Delta t}(\alpha_0 \bar{\boldsymbol{u}}^{n+1} + \sum_{q=1}^{q=Q} \alpha_q \bar{\tilde{\boldsymbol{u}}}^{n+1-q}) \tag{10}$$

The closure problem now reads: Determine the $\bar{\tilde{\boldsymbol{u}}}^{n+1-q}$ from the $\bar{\boldsymbol{u}}^{n+1-q}$.

With T for the transport operator such that: $\tilde{u}_i^{n+1-q} = T u_i^{n+1-q}$, the most immediate DTF approach consists in applying successively the defiltering, transport and filtering operators to each component of the velocity field:

$$\bar{\tilde{\boldsymbol{u}}}^{n+1-q} = G\,T\,G^+ \bar{\boldsymbol{u}}^{n+1-q} \tag{11}$$

where T depends on the "defiltered velocity", i.e. $T = T(G^+ \bar{\boldsymbol{u}})$. Hereafter we refer to this three steps algorithm by DTF.1.

However one can check that DTF.1 yields a consistency failure: Let $\Delta t \to 0$, so that $T \to 1$, then, since G^+ is only an approximate inverse of G:

$$(\alpha_0 + \sum_{q=1}^{q=Q} \alpha_q G\, G^+)\bar{\boldsymbol{u}}^{n+1} \neq 0 \tag{12}$$

which means that the material derivative blows up for $\Delta t = 0$.

Such a failure may be overcome by using:

$$\tilde{\bar{\boldsymbol{u}}}^{n+1-q} = (G\, T\, G^+ + 1 - G\, G^+)\, \bar{\boldsymbol{u}}^{n+1-q} \tag{13}$$

which results from substracting from eq. (11) the "equality":

$$\bar{\boldsymbol{u}}^{n+1-q} \approx G\, G^+\, \bar{\boldsymbol{u}}^{n+1-q} \tag{14}$$

The corresponding algorithm is called hereafter DTF.2.

The algorithms DTF.1 and DTF.2 have been implemented in two 3D DNS solvers: (i) a spectral collocation solver (Chebyshev-Chebyshev-Fourier) and (ii) a Fourier-Legendre spectral element solver. Both solvers make use at each time-cycle of a two-step algorithm. First, in a "transport step", one solves the Q auxiliary problems ($q = 1, \cdots, Q$):

$$\begin{cases} \partial_t \phi + \boldsymbol{u} \cdot \nabla \phi = 0 \\ \phi(t_{n+1-q}) = u_i^{n+1-q} \end{cases} \tag{15}$$

$$Then: \quad \tilde{u_i}^{n+1-q} = \phi(t_{n+1}) \tag{16}$$

To this end we use a RK4 (Fourth order Runge Kutta) scheme with sub-time cycling (see [25] for details).

Second, one has to compute $\bar{\boldsymbol{u}}^{n+1}$ by solving the generalized Stokes problem:

$$\begin{cases} \dfrac{\alpha_0}{\Delta t}\bar{\boldsymbol{u}}^{n+1} + \nabla \bar{p}^{n+1} - \nu \nabla^2 \bar{\boldsymbol{u}}^{n+1} = -\dfrac{1}{\Delta t} \displaystyle\sum_{q=1}^{q=Q} \alpha_q \tilde{\bar{\boldsymbol{u}}}^{n+1-q} \\ \nabla \cdot \bar{\boldsymbol{u}}^{n+1} = 0 \end{cases} \tag{17}$$

which splits into a set of 2D-like problems, handled with the Chebyshev or the spectral element approximation. Hereafter we focus on the Chebyshev solver (mono-domain version of [19]), for which numerical results are given in Section 4.

Note that since a RK scheme is used for the transport step:

$$\tilde{\boldsymbol{u}}^{n+1-q} = \boldsymbol{u}^{n+1-q} + \Delta t \sum_k \mathbf{R}_k \tag{18}$$

where the $\mathbf{R}_k$ denote the terms of the RK scheme. Then DTF.1 and DTF.2 yield to use the following non-consistent and consistent forms respectively:

$$\tilde{\bar{\boldsymbol{u}}}^{n+1-q} = GG^+\bar{\boldsymbol{u}}^{n+1-q} + \Delta t\, G \sum_k \mathbf{R}_k \tag{19}$$

$$\tilde{\bar{\boldsymbol{u}}}^{n+1-q} = \bar{\boldsymbol{u}}^{n+1-q} + \Delta t\, G \sum_k \mathbf{R}_k \tag{20}$$

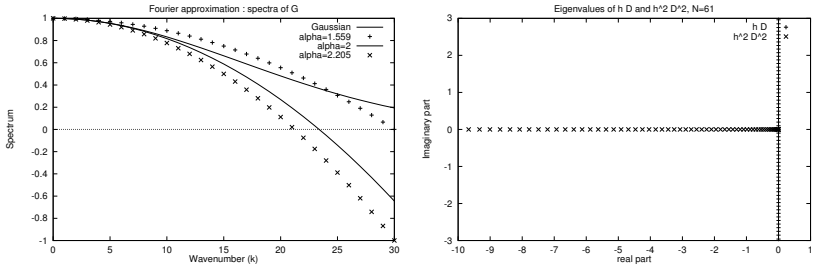

Figure 1: left: 1 D periodic case, Fourier spectra of G for $\alpha = \{1.559, 2, 2.205\}$ and of the Gaussian filter; right: 1D non-periodic case, eigenvalues of the Chebyshev approximations of $h\partial_x$ and $h^2\partial_x^2$.

3 Filtering and defiltering procedures

The main ingredients of the DTF algorithms are the filtering and defiltering operators. As mentioned in introduction, following [12] we plan to use differential operators which are expected to approximate the Gaussian or ("box") filter and of its inversion (see eq. (7)). In this Section we present a spectral analysis of such operators in the 1D periodic and non-periodic cases, using a Fourier and a Chebyshev approximation respectively.

1D periodic case (Fourier approximation):

In Fig. 1 (left) we present the Fourier spectra of G, say $\hat{G}$, obtained for different values of the ratio $\alpha = \Delta/h$. Such curves are parabola of equations:

$$\hat{G}_k = 1 - \frac{\alpha^2\pi^2}{24}(\frac{k}{K})^2 \tag{21}$$

where K is the number of Fourier modes ($K = 30$ in Fig. 1).

Of course the Fourier spectrum of G^+ is the one obtained by symmetry with respect to $\hat{G} = 1$. We have also plotted the Fourier spectrum of the Gaussian filter that is to be approximated: One observes that with $\alpha = 2$ the approximation is only valid for the low frequencies. More precisely one can check that:

- with $\alpha = 2$, if $k/K > 0.8$ then $\hat{G}_k < 0$, i.e. G is not a filtering operator,
- $\min(\hat{G}_k) \geq 0$ requires $\alpha \leq 1.559$,
- if $\alpha > 2.205$, $\max|\hat{G}_k| > 1$, i.e. $||G||^n \longrightarrow \infty$ as $n \longrightarrow \infty$.

Moreover, the stability of the DTF.1 algorithm is governed by the operator $G\,G^+$, since if $\Delta t \to 0$, $T \to 1$. It can be easily checked that :

- if $\alpha > 1.854$, then $||G\,G^+||^n \longrightarrow \infty$ with n.

Finally, it must be stressed that to maintain these properties in 3D the operator G must be defined as the tensorial product of 1D operators. With $G = 1 + A$, it turns out that G is really a filtering operator only if $\alpha < 0.9$ and that the stability constraint reads $\alpha < 1.071$.

1D non-periodic case (Chebyshev approximation):

To handle the non-periodic case we proceed to an eigenvalue analysis of the Chebyshev approximation of G. To this end we restrict the definition domain of

G to the space P_N of polynomials of degree N and use the usual Gauss-Lobatto-Chebyshev grid, so that G is now a matrix of dimension $(N+1)\times(N+1)$. The eigenvalues of G, say λ_i, write:

$$\lambda_i = 1 + \frac{\alpha^2}{24}\mu_i \tag{22}$$

where the μ_i are the eigenvalues of the discrete form of $h^2\partial_x^2$.

In Fig. 1 (right) we have plotted the eigenvalues of the Chebyshev approximations of $h\partial_x$ and $h^2\partial_x^2$, with h a local mesh size obtained through the collocation grid: $h(x_i) = (x_{i+1} - x_{i-1})/2$, $0 < i < N$, and $h(x_0) = h(x_N) = x_1 - x_0$, where $\{x_i, i = 0, \cdots, N\}$ is the set of the Gauss-Lobatto-Chebyshev points, i.e. $x_i = -\cos z_i, \quad z_i = i\,\delta z, \quad \delta z = \pi/N$. One observes that (i) for $h\partial_x$ the eigenvalues are imaginary and that (ii) the μ_i are real non positive.

The critical values of α can be easily determined:

- $0 \le \lambda_i \le 1 \quad \Longleftrightarrow \quad \alpha \le \sqrt{24/\max(-\mu_i)}$,
- $|\lambda_i| \le 1 \quad \Longleftrightarrow \quad \alpha \le \sqrt{48/\max(-\mu_i)}$.

N	61	122	244	488
$\max(-\mu_i)$	9.672	9.777	9.825	9.848

Table 1

Table 1 lists the values of $\max(-\mu_i)$, i.e. of the spectral radius of the Chebyshev approximation of $h^2\partial_x^2$, for different values of N. One observes that the dependence on N is weak. Moreover, in the limit $N = \infty$, $\max(-\mu_i) = \pi^2$ so that the Chebyshev and Fourier critical α are the same. Thus, for $N = 488$ we find that G is actually a filtering operator if $\alpha < 1.561$.

Numerical tests on stability of the combined filtering-defiltering procedure using both spectral element and Chebyshev methods were in good agreement with these estimated critical values of α.

Remark: For large values of N the above results can be interpreted from the relations:

$$h\,\partial_x \approx (\frac{dx}{dz}\,\delta z)(\frac{dz}{dx}\,\partial_z) = \delta z\;\partial_z = \frac{\pi}{N}\partial_z \tag{23}$$

$$h^2\partial_x^2 \approx \delta z^2(\partial_z^2 + \frac{d^2z}{dx^2}(\frac{dx}{dz})^2\partial_z) = \frac{\pi^2}{N^2}(\partial_z^2 - \frac{1}{\tan(z)}\partial_z). \tag{24}$$

Filtering in Fourier space:

The previous analysis gives rise to the idea of filtering in Fourier space, i.e to apply a filter of constant width to the 2π-periodic function $u(-\cos(z)), z \in \mathbb{R}$.

Of course, such an approach shows the main advantage that the spectrum of G may be directly defined. Moreover, one gets rid of the sensitive problem of near-wall filtering, assuming implicitly that the filter-width in normal direction vanishes at the wall. Hereafter, in order to recover the filtering property we use $\hat{G}'_k = \max(\hat{G}_k, 0)$, i.e. the convolution product of G with a spectral cutoff filter. Such a cutoff includes a partial de-aliasing effect.

One should remark that:

- filtering for non-equidistant grids is defined in a related way in [8],
- the method can be generalized as soon as $x_i = H(i\delta z)$, with H a smooth, pair and $2\,\pi$-periodic mapping, as it is e.g. the case for the Gauss-Lobatto-Legendre grid.

4 Preliminary numerical experiments: Analysis and improvements

The first numerical experiments have shown that (i) DTF.1 is too much dissipative and yields time-step dependent results (consistency problem) whereas (ii) DTF.2 is not dissipative and so not stable for reasonable values of the time-step.

To point out the dissipative feature of DTF.1, let us assume a BD1 approximation of the material derivative and use a RK scheme for the transport step. Then, DTF.1 yields for the momentum equation:

$$\frac{\bar{\boldsymbol{u}}^{n+1} - G\,G^{+}\bar{\boldsymbol{u}}^{n}}{\Delta t} - G\sum_{k}\mathbf{R}_{k} + \nabla\bar{p}^{n+1} - \nu\nabla^{2}\bar{\boldsymbol{u}}^{n+1} = 0 \tag{25}$$

where again the $\mathbf{R}_k$ are the terms that appear in the RK scheme. Such an equation also writes:

$$\frac{\bar{\boldsymbol{u}}^{n+1} - \bar{\boldsymbol{u}}^{n}}{\Delta t} - G\sum_{k}\mathbf{R}_{k} + \nabla\bar{p}^{n+1} - \nu\nabla^{2}\bar{\boldsymbol{u}}^{n+1} = -\frac{1}{\Delta t}(1 - G\,G^{+})\bar{\boldsymbol{u}}^{n} \tag{26}$$

Clearly the right hand side term is dissipative but, as expected, depends on the time-step.

However, it is of interest to outline that such a dissipative term is close to the one introduced in [22]. Even more, if one combines DTF.1 and DTF.2, for the computation of the $\bar{\bar{\boldsymbol{u}}}^{n+1-q}$, by using weighted coefficients equal to $\chi\Delta t$ and $(1 - \chi\Delta t)$ respectively, then one obtains:

$$\frac{\bar{\boldsymbol{u}}^{n+1} - \bar{\boldsymbol{u}}^{n}}{\Delta t} - G\sum_{k}\mathbf{R}_{k} + \nabla\bar{p}^{n+1} - \nu\nabla^{2}\bar{\boldsymbol{u}}^{n+1} = -\chi(1 - G\,G^{+})\bar{\boldsymbol{u}}^{n} \tag{27}$$

which exactly shows the dissipative term of [22]. The time-scheme is now consistent, but it appears a new parameter: χ. In [22] a dynamic modeling is used to adjust the value of this parameter.

In order to overcome the lack of dissipation of the DTF.2 algorithm, we suggest using stabilization techniques. Especially,

- the spectral vanishing viscosity (SV) method, introduced in [16, 23] for conservation laws. It consists of introducing a viscous term acting only the highest frequencies. Let us mention that the SV method was successfully checked in [11], in the framework of the so-called MILES (Monotone Integrated LES) appoach, when no SGS modeling is used (see e.g. [6]);

- the filter-based stabilization technique proposed in [4]. Stabilization is obtained by interpolation, at each time-step, of the solution, say in the polynomial space P_N, onto the Gauss-Lobatto grid of the polynomial space P_{N-1}.

To check the DTF.2 algorithm associated to the SV method, we have used the Chebyshev collocation solver for the computation of the wake behind a circular cylinder. The Reynolds number, based on the mean flow velocity and the cylinder diameter, is equal to $Re = 1000$. This value corresponds to the lower part ($350 \leq Re \leq 1500$) of the turbulent sub-critical regime ($350 \leq Re \leq 300000$). The flow is computed in the domain $\Omega =]-2; 4[\times]-3; 3[\times]0; 4[$, the cylinder axis being located at $x = 0, y \approx 0$. A "smoothed penalty technique" [5] is used

to model the cylinder, i.e. a penalty term is introduced in the momentum equation to cancel the velocity inside the cylinder and its characteristic function is filtered ("raised cosine filter") to weaken the Gibbs phenomenon. At the outflow boundary of the computational domain we impose to the velocity components an advection equation based on the mean flow velocity. Free-slip boundary conditions are used at $y = \pm 3$ and the z-direction is assumed homogeneous. The calculation parameters are $Q = 2$, $N_x = 61, N_y = 61, N_z = 40$ and $\Delta t = 5.10^{-3}$. No-sub-cycling is used in the transport step. The spectral viscosity is increased smoothly, as suggested in [16], from 0 to the inverse of the number of Chebyshev or Fourier modes in the upper half part of the Chebyshev and Fourier spectra.

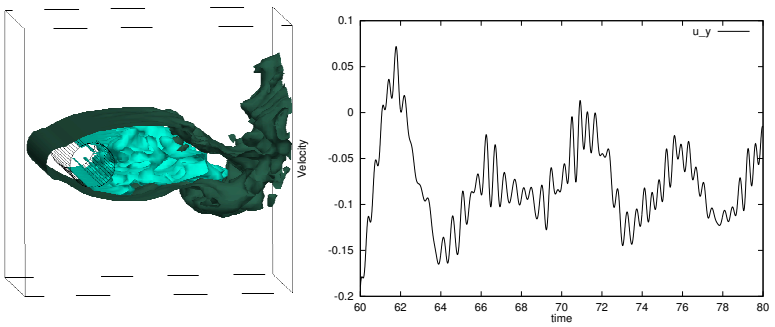

Figure 2: DTF2+SV, left: $u_x = \{0, 0.8\}$ at $t = 80$; right: history plot of u_y downstream of the cylinder.

Fig. 2 points out the turbulent feature of the flow: Visualization of the streamwise component shows that the flow is fully 3D and the crosswise component at a point downwards the cylinder is quickly oscillating. However, one can discern a dominant frequency yielding a Strouhal number $St \approx 0.21$, which is in agreement with the numerical and experimental results presented in [10, 24] respectively.

In Fig. 3 we have plotted isovalues of the streamwise component of the velocity in the planes $z = 2$ and $y = 0$, and also the spanwise component of the vorticity for $z = 2$, at times corresponding approximatively to one vortex shedding period. Such results point out that the recirculation length is less than two cylinder diameters. Also the instantaneous vorticity plots, shown without any post-processing, exhibit the expected separating shear layers downstream of the cylinder.

5 Conclusion

Using high-order methods for the LES of turbulent flows should permit to find out numerical solutions not "polluted" by approximation errors. With this goal, DTF algorithms have been proposed and implemented in spectral solvers. Basically they are of the scale similarity type, but improved through the use of an ADM. The main idea is to take benefit of a semi-Lagrangian formulation to handle with an efficient explicit algorithm the additional terms arising in the Navier-Stokes equations. It has been pointed out that for the filtering and

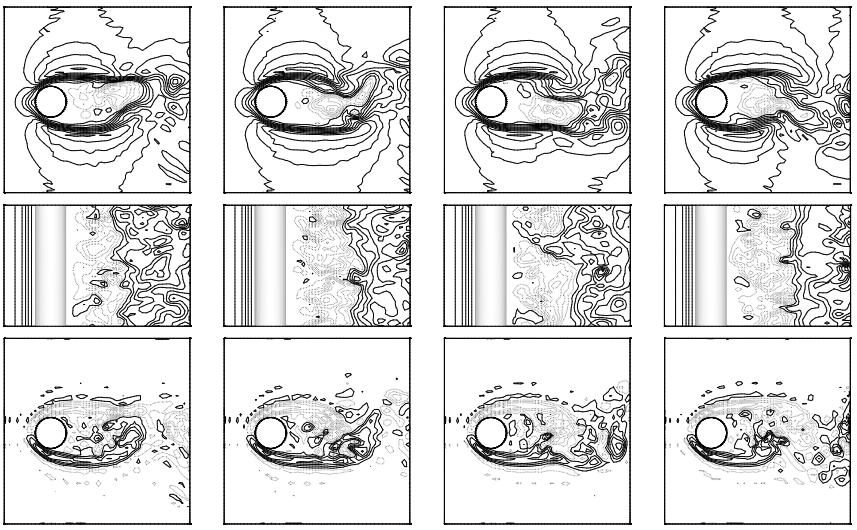

Figure 3: DTF2+SV, $u_x(z = 2)$ (top), $u_x(y = 0)$ (medium) and $\omega_z(z = 2)$ (bottom) at $t = \{77, 78, 79, 80\}$. Negative values are in dashed lines, $\delta u_x = 0.2$ and $\delta\omega_z = 2$.

defiltering procedures, using approximations of the convolution and deconvolution operators with differential ones must be done with care. Also it has been shown that filtering-defiltering in Fourier space could be of interest when Gauss-Lobatto type computational grids are concerned.

Just like other ADM, the DTF algorithms need additional regularization: This can be achieved through the use of stabilization techniques, like the spectral vanishing viscosity method. The results that have been presented are preliminary ones. The aim is now an improvement of the algorithms and "*a posteriori*" tests to check the turbulence features of the computed flows.

Aknowledgments This study was supported by the AFCRST (Association Franco-Chinoise pour la Recherche Scientifique et Technique). We are grateful to J. Ferziger for fruitful discussions during his stay in the lab. J.A. Dieudonné (September 2000). We also thank J.M. Lacroix for his helpful technical support.

References

[1] Bardina, J. et al. (1983). Improved turbulence models based on large eddy simulation of homogeneous incompressible turbulence, Stanford University, Report TF-19.

[2] Domaradzki, J.A., and Saiki, E.M. (1997). A subgrid-scale model based on the estimation of unresolved scales of turbulence, *Phys. Fluids*, **9**(7), 2148-2164.

[3] Geurt, B.J. (1997). Inverse modeling for large-eddy simulation, *Phys.Fluids*, **9**(12), 3585-3587.

[4] Fischer, P., and Mullen, J. (2001). Filter-based stabilization of spectral element methods, *C. R. Acad. Sci. Paris*, **332** (1), 265-270.

[5] Forestier, M.Y. et al. (2000). Computations of 3D wakes in stratified fluids, *Computational Fluid Dynamics Conference ECCOMAS 2000*, proc. in CD.

[6] Garnier, E. et al. (1999). On the use of shock-capturing schemes for large-eddy simulation, *J. Comp. Phys.*, **153**, 273-311.

[7] Germano, M. et al. (1991). A dynamic sub-grid scale eddy viscosity model. *Phys. Fluids*, **3** (7), 1760-1765.

[8] Ghosal, S., and Moin, P. (1995).The basic equations for the large-eddy simulation of turbulent flows in complex geometry, *J. Comp. Phys.*, **118**, 24-37.

[9] Ghosal, S. (1996). An analysis of numerical errors in large-eddy simulation of turbulence, *J. Comp. Phys.*, **125**, 187-206.

[10] Henderson, R.D. (1997). Nonlinear dynamics and pattern formation in turbulent wake transition, *J. Fluid Mech.*, **352**, 65-112.

[11] Karamanos, G.S., and Karniadakis, G.E. (2000). A spectral vanishing viscosity method for large-eddy simulation, *J. Comp. Phys.*, **163**, 22-50.

[12] Katopodes, F.V. et al. (2000). A theory for the subfilter-scale model in large-eddy simulation, Stanford University, Tech. Report 2000-K1.

[13] Kravchenko, A.G., and Moin, P. (1997). On the effect of numerical errors in large-eddy simulations of turbulent flows, *J. Comp. Phys.*, **131**, 312-322.

[14] Lesieur, M. (1990). *Turbulence in fluids*, Kluwer Academic, Dordrecht.

[15] Lesieur, M., and Métais, O. (1996). New trends in large-eddy simulation of turbulence, *Annu.Rev.Fluid Mech.*, **28**, 45-82.

[16] Maday, Y. et al. (1993). Legendre pseudo-spectral viscosity method for nonlinear conservation laws, *SIAM J. Numer. Anal.*, **30** (2), 321-342.

[17] Maday, Y., et al. (1990). An operator-integration-factor splitting method for time-dependent problems: application to incompressible fluid flow, *J.of Sci. Comp.*, **5**(4), 263-292.

[18] Phillips, R.M. and Phillips, T.N. (2000). Flow past a cylinder using a semi-Lagrangian spectral element method, *Appl. Num. Math*, **33**, 251-257.

[19] Sabbah, C. and Pasquetti, R. (1998). A divergence-free multi-domain spectral solver of the Navier-Stokes equations in geometries of high aspect ratio, *J. Comput. Phys.*, **139**, 359-379.

[20] Sagaut, P. (1998), *Introduction à la simulation des grandes échelles pour les écoulements de fluide incompressible*, Mathématiques & Applications, Springer.

[21] Stolz, S., and Adams, N.A. (1999). An approximate deconvolution procedure for large-eddy simulation, *Phys.Fluids*, **11**(7), 1699-1701.

[22] Stolz, S. et al. (2001). An approximate deconvolution model for large-eddy simulation with application to incompressible wall-bounded flows, *Phys.Fluids*, **13** (4), 997-1015.

[23] Tadmor, E. (1989). Convergence of spectral methods for nonlinear conservation laws, *SIAM J. Numer. Anal.*, **26** (1), 30-44.

[24] Williamson, C.H.K. (1989). Oblique and parallel modes of vortex shedding in the wake of a circular cylinder at low Reynolds numbers, *J. Fluid Mech.*, **206**, 579-627.

[25] Xu, C.J., and Pasquetti, R. (2001). On the efficiency of semi-implicit and semi-Lagrangian spectral methods for the calculation of incompressible flows, *Inter. J. Numer. Meth. Fluids*, **35**, 319-340.